

Photocatalytic properties of $\text{Co}_3\text{O}_4/\text{LiCoO}_2$ recycled from spent lithium-ion batteries using citric acid as leaching agent



I.L. Santana, T.F.M. Moreira, M.F.F. Lelis, M.B.J.G. Freitas*

Federal University of Espírito Santo, Av. Fernando Ferrari, 514, Vitória, ES, CEP:29075-910, Brazil

HIGHLIGHTS

- Synthesis a mixture of $\text{Co}_3\text{O}_4/\text{LiCoO}_2$ from spent Li-ion batteries.
- Citric acid for leaching of the cathodes of the spent Li-ion batteries.
- $\text{Co}_3\text{O}_4/\text{LiCoO}_2$ as catalysts in the photodegradation of the methylene blue dye.

ARTICLE INFO

Article history:

Received 13 October 2016

Received in revised form

30 December 2016

Accepted 1 January 2017

Available online 5 January 2017

Keywords:

Recycling

Spent lithium-ion batteries

Cobalt oxide

Lithium cobalt oxide

Citric acid

ABSTRACT

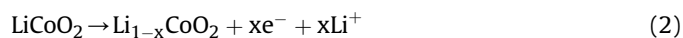
In this work, cobalt and lithium from the cathodes of spent lithium-ion batteries were recycled to synthesize a mixture of Co_3O_4 and LiCoO_2 . The positive electrode was leached with citric acid in the green recycling. After being heated to 85 °C, the leaching solution formed a pink sol, and after being dried at 120 °C for 24 h, it formed a gel, which is a precursor material for Co_3O_4 and LiCoO_2 synthesis. A mixture of Co_3O_4 and LT- LiCoO_2 was obtained after the calcination of the precursor material at 450 °C for 3 h. The photocatalytic properties of the Co_3O_4 and LiCoO_2 were tested in the discoloration of methylene blue dye. The discoloration efficiency of methylene blue dye in the presence of Co_3O_4 and LiCoO_2 was 90% after 10 h and 100% after 24 h of heterogeneous catalysis. The contribution of this work is that it presents a means to produce valuable materials with photocatalytic properties from recycled batteries through a spent Li-ion battery recycling process without polluting the environment.

© 2017 Elsevier B.V. All rights reserved.

1. Introduction

Lithium-ion batteries possess a high energy density, a low self-discharge rate, and a long life cycle compared to Ni-MH or Ni-Cd batteries. Therefore, they have become a dominant power source for portable electronic devices and hybrid vehicles [1]. Li-ion batteries are made of a graphite anode, a non-aqueous liquid electrolyte, and a cathode of an intercalation oxide. Intercalations of mixed oxides used in cathode composition have the following compositions: LiCoO_2 , $\text{LiCo}_{1-x}\text{Ni}_x\text{O}_2$, $\text{LiMn}_{1.5}\text{Ni}_{0.42}\text{Zn}_{0.08}\text{O}_4$ and $\text{Li}(\text{Ni}_{1/3}\text{Mn}_{1/3}\text{Co}_{1/3})\text{O}_2$. LiCoO_2 is the most commonly used material for Li-ion batteries because of its high energy density, high operating voltage, and good electrochemical performance. During the charging process, lithium ions de-intercalate from layered LiCoO_2 , pass through electrolytes, and intercalate in layered graphite [2–5].

LiCoO_2 can exist in two structures: low-temperature (LT- LiCoO_2) and high-temperature (HT- LiCoO_2). LT- LiCoO_2 has a spinel-type structure, and it is obtained at temperatures below 500 °C. HT- LiCoO_2 has a hexagonal and lamellar structure, and it is obtained at temperatures above 500 °C [6]. Eqs. (1) and (2) describe the charging process in the anode and cathode of Li-ion batteries:



The annual worldwide market for rechargeable lithium batteries is estimated at \$10 billion (US), and it continues to grow. Spent Li-ion batteries generate large amounts of hazardous waste and cause the loss of valuable metals, such as lithium and cobalt [2,7]. The cobalt used in Li-ion battery manufacturing is 25% of the global demand for cobalt [4]. According to the London Metal Exchange (LME), the cobalt price in January 2016 was \$22.50/kg⁻¹ (US). Furthermore, cobalt is toxic to the environment, and lithium cobalt

* Corresponding author.

E-mail address: marcosbjg@gmail.com (M.B.J.G. Freitas).

oxide waste needs appropriate management. Lithium is a valuable metal and important to many industrial applications, but it can create environmental problems because it is chemically reactive with H_2O , N_2 , and O_2 [8]. In addition, a Li-ion battery's electrolytes contain toxic organic compounds and LiOH , which is extremely corrosive and causes damage to the environment [4]. In general, lithium and cobalt represent 5–7 wt% and 5–20 wt% of a Li-ion battery's content, respectively [9].

Modern society is concerned with the environment and the environmental damage caused by spent Li-ion batteries. Therefore, it is necessary to develop new methodologies and technologies to recycle these spent batteries in an eco-friendly way. Li-ion batteries can be recycled by pyrometallurgical, bio-hydrometallurgical, or hydrometallurgical processes. The pyrometallurgical process is characterized by high energy consumption, and it releases a large amount of toxic gases into atmosphere. The bio-hydrometallurgical process is efficient, but it requires a very long time to recycle Li-ion batteries. The hydrometallurgical process offers advantages such as low energy consumption, minimal gas emission, and recovery of pure metal [10]. This process uses strong inorganic acids to recover 99% of the cobalt and nearly 100% of the lithium from spent Li-ion batteries. During leaching, the inorganic acids release Cl_2 , SO_3 , and NO_x , and the leaching solutions need chemical treatment. Organic acids, on the other hand, are an alternative to avoid the secondary pollution that strong inorganic acids produce. Organic acids have positive characteristics during the hydrometallurgical process: they easily and naturally degrade, and they do not release toxic gases. Citric acid has a high leaching efficiency and a low price; therefore, it is commonly used as a leaching agent for the hydrometallurgical recovery of cobalt and lithium from spent Li-ion batteries [9,11,12]. Once recovered by the hydrometallurgical process, the cobalt and lithium of spent batteries can be reused to obtain a variety of cobalt materials in the recycling process. Metallic cobalt, Co_3O_4 , and LiCoO_2 can be obtained using techniques such as electrodeposition and chemical precipitation [1,12–14].

In the present study, citric acid was used to recover cobalt and lithium from spent Li-ion batteries. The cobalt and lithium were recycled to synthesize a mixture of Co_3O_4 and LiCoO_2 after calcination of the precursor material. The photocatalytic properties of the Co_3O_4 and LiCoO_2 were tested in the discoloration of the methylene blue dye. The characterization of the recycled materials was performed by employing X-ray diffraction (XRD), scanning electronic microscopy (SEM), infrared spectroscopy (IR), and Raman spectroscopy.

2. Experimental

2.1. Cathode separation and leaching using citric acid

Spent 3.7 V Li-ion batteries from a Samsung[®] cell phone (model EB600BE) were used in this study. The batteries were completely discharged and manually dismantled. Plastic and steel cases were removed from the cells, and the anodes and cathodes were extracted. Cathodic active materials were detached from the supports and dried at 120 °C for 24 h to eliminate organic compounds. Finally, the active material was washed with distilled water and dried at 60 °C. Citric acid was used to dissolve Co and Li from the batteries, and H_2O_2 was employed as a reducing agent. The experimental conditions used for leaching were as follows: 2.0 mol L^{-1} of citric acid, temperature of 80 °C, time of 90 min, a liquid-solid ratio of 20 g L^{-1} , and 3 v/v% of H_2O_2 30 v/v%.

2.2. Synthesis of Co_3O_4 and LiCoO_2 from spent Li-ion batteries

For the synthesis of the recycled materials, 50 mL of the cathode

material leaching solution was heated to 85 °C and kept in constant agitation for 5 h. The leaching solution formed a pink sol after being heated to 85 °C. The pink sol was dried at 120 °C for 24 h, and it formed a gel, which is a precursor material for lithium cobalt oxide synthesis. Fig. 1 shows a pink sol and a gel (precursor material). We obtained the lithium cobalt oxide after the calcination of the precursor material at 450 °C for 3 h. This yielded a Co_3O_4 and LiCoO_2 mixture.

2.3. Application of Co_3O_4 and LiCoO_2 in methylene blue dye discoloration

Heterogeneous catalysis was used for the discoloration of methylene blue dye. The dye solution was prepared in a concentration of 3 mg L^{-1} with the addition of 3 mL of H_2O_2 . The pH of the solution was adjusted to 3 using sulfuric acid. For catalysis, 3 mg of catalyst powders was added to 50 mL of the dye solution. Photocatalysis was held in a T&M Instruments cabin light using 20-W UV light radiation (Phillips). Discoloration of the methylene blue dye was analyzed and measured with a UV–visible spectrophotometer at wavelengths of 613 nm and 664 nm. The methylene blue dye showed a maximum absorption band in the visible region at 664 nm with a small shoulder at 613 nm. The conjugation system between the two dimethylamine-substituted aromatic rings through the sulfur and nitrogen is responsible for the absorbance at 664 nm. The small shoulder at 613 nm is due to the absorbance of dye dimer, whereas the substituted benzene rings have their absorption bands in the ultraviolet region. Methylene blue is a cationic dye with a dimer responsible for coloration, as shown in Fig. 2.

2.4. Characterization of a cathode from spent Li-ion batteries and the recycled materials

Cathodic active materials and recycled cobalt oxide powders were submitted to XRD using Shimadzu XRD-600 equipment, model 20013, with $\text{CuK}\alpha$ radiation ($\lambda = 1.5418 \text{ \AA}$) and Bruker equipment, model D2 Phaser, with $\text{CuK}\alpha$ radiation ($\lambda = 1.5406 \text{ \AA}$) at a rate of 2° min^{-1} . Characteristic peaks were analyzed with a Crystallographica Search Match[®] program.

Micrographs were carried out using a JEOL 6610LV scanning electron microscope. The composition of cathodic active and recycled material powders were determined by Raman spectroscopy, module AFM Alpha 300 WITEC, with a laser of 532 nm utilized as an excitation source.

Thermal analyses of the precursor material were performed with SDT Q600 V20.9 Build 20 module DSC-TGA standard equipment, with an air flow of 100 mL min^{-1} , a heating rate of 10 °C min^{-1} , and a maximum temperature of 1000 °C.

Dye discoloration was monitored by atomic absorbance and was recorded with a HACH UV–visible spectrophotometer model DR5000.

3. Results and discussion

3.1. Characterization of spent Li-ion batteries, precursor material, and recycled materials

Fig. 3A represents the typical X-ray diffraction spectrum for the cathode of a spent Samsung[®] Li-ion battery. According to the Crystallographica Search Match[®] program, the assigned peaks have similar characteristics to higher temperature LiCoO_2 (HT- LiCoO_2) (card 44–145). The LiCoO_2 used in Li-ion batteries is usually prepared by solid-state reaction, at higher temperatures (800 °C) and for a longer time (8 h).



Fig. 1. (a) Pink sol, (b) Dried gel, which is a precursor material for lithium cobalt oxide synthesis.

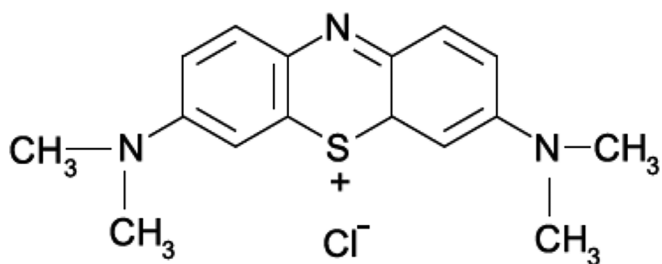


Fig. 2. Methylene blue dye molecule.

Fig. 3B represents the Raman spectroscopy of spent battery cathodes. The most intensive bands at 590 cm^{-1} and 478 cm^{-1} in the Raman spectrum of spent batteries are characteristic of HT-LiCoO₂ [15]. The band at 478 cm^{-1} is attributed to the E_g mode, related to the stretching of the Co–O bonds, and the band at 588 cm^{-1} is attributed to the A_{1g} mode. The band at 679 cm^{-1} is characteristic of the Co₃O₄ formed by the decomposition reaction of LiCoO₂ [16]. During battery operation, when the lithium fraction in LiCoO₂ becomes less than 0.50, the decomposition of LiCoO₂ starts. The formation of Co₃O₄ represents one of the main reasons for the loss of capacity in Li-ion batteries. Co₃O₄ reacts by adsorbing the Li⁺ irreversibly in their structure. Eq. (3) represents the decomposition of Li_{0.50}CoO₂ into O₂ and Co₃O₄ [17].

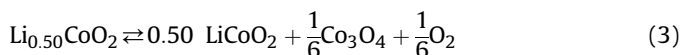


Fig. 3C shows the micrographs for the cathode of a spent Li-ion battery. The spent HT-LiCoO₂ can be seen in the inner region of the agglomerated crystals, and, within the agglomeration, there is porosity for electrolyte penetration. Cracks can be seen on the surface of the spent HT-LiCoO₂.

Thermogravimetry (TG) and differential scanning calorimetry (DSC) analyses of the precursor material are shown in Fig. 4. The TG analysis indicates that there is a weight loss of 90 wt% when the temperature is between $200\text{ }^{\circ}\text{C}$ and $425\text{ }^{\circ}\text{C}$ due to the organic material calcination. When the temperature is between $450\text{ }^{\circ}\text{C}$ and $1000\text{ }^{\circ}\text{C}$ in the TG, there is no weight loss. In the DSC plot, an exothermic process between $365\text{ }^{\circ}\text{C}$ and $412\text{ }^{\circ}\text{C}$ can be observed; it is assigned to the formation of Co₃O₄ and LT-LiCoO₂. An endothermic process occurs between $412\text{ }^{\circ}\text{C}$ and $842\text{ }^{\circ}\text{C}$ due to a solid-state reaction for HT-LiCoO₂ formation, where lithium intercalates in the layered Co₃O₄ [18–20]. The calcination temperature of $450\text{ }^{\circ}\text{C}$ was chosen in this study after considering TG and DSC analyses.

An IR spectra of the precursor material and material calcined at $450\text{ }^{\circ}\text{C}$ is shown in Fig. 5. The narrow and broad bands from 3210 cm^{-1} to 3505 cm^{-1} are from the stretching vibrations of OH in the citrate precursor. The narrow band at 3287 cm^{-1} reveals the

formation of a complex network of hydrogen bonding in the citric acid. Bands in the $1160\text{--}1100\text{ cm}^{-1}$ spectral range correspond to the bending and stretching vibrations of OH and C–O(H) for tertiary alcohols. The band at about 3400 cm^{-1} can be attributed to the crystal and/or the coordination water for lithium and cobalt citrates. The band at 1404 cm^{-1} is attributed to the vibrations of coordinated carboxyls, and the band at 1700 cm^{-1} corresponds to carbonyl [18,19,21,22]. After calcination, small amounts of organic matter remain in material calcined at $450\text{ }^{\circ}\text{C}$.

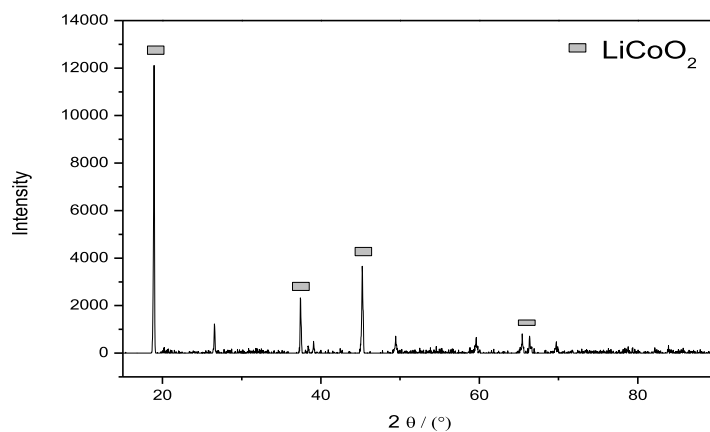
Fig. 6A represents the typical X-ray diffraction spectrum for recycled cobalt oxide material. According to the Crystallographica Search Match® program, the recycled material calcined at $450\text{ }^{\circ}\text{C}$ is a mixture of cobalt oxide Co₃O₄ (card 43–1003) and LiCoO₂ (card 44–145).

A Raman spectroscopy was made to complement the XRD characterization. Fig. 6B represents the Raman spectroscopy of recycled materials. Recycled material calcined at $450\text{ }^{\circ}\text{C}$ has the most intensive Raman bands at 660 cm^{-1} . This band is characteristic of cubic spinel Co₃O₄ [23–26]. The presence of the band at 660 cm^{-1} was also verified by H. Porthault et al. [23] and Christopher et al. [24]. The authors attributed the band at 660 cm^{-1} to Co₃O₄. This assignment was based on the synthesis of LT-LiCoO₂ from Co₃O₄. A part of Co₃O₄ that does not react with Li⁺ ions remains as an impurity in the LT-LiCoO₂ samples. Small bands at 190 cm^{-1} and 506 cm^{-1} are also characteristic of spinel Co₃O₄. The band at 458 cm^{-1} is attributed to spinel LT-LiCoO₂, and the band at 600 cm^{-1} can be attributed to both LT-LiCoO₂ and Co₃O₄. The band at 600 cm^{-1} is assigned to Co–O stretching modes of the CoO₆ octahedral, while the lower frequency bands (458 cm^{-1}) are assigned primarily to O–Co–O bending motions. The recycled material calcined at $450\text{ }^{\circ}\text{C}$ is a mixture of LT-LiCoO₂ and Co₃O₄ compounds [23–26].

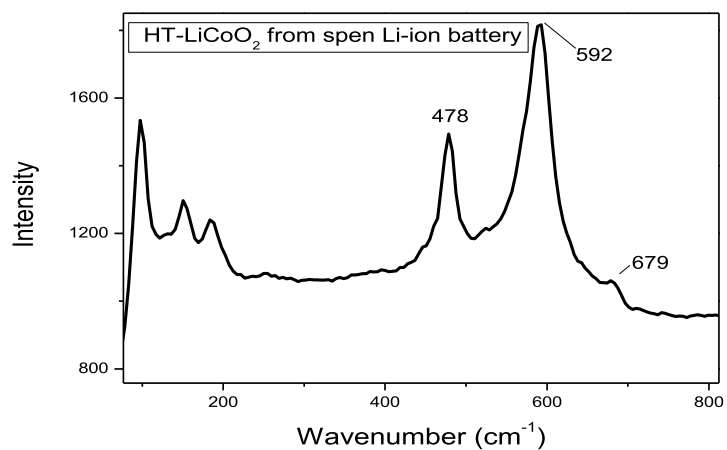
Fig. 6C shows the micrograph for the recycled cobalt oxides synthesized at $450\text{ }^{\circ}\text{C}$ (LiCoO₂ and Co₃O₄). The recycled materials have porosity and agglomerated particles.

3.2. Application of Co₃O₄ and LiCoO₂ as catalysts of the methylene blue dye degradation

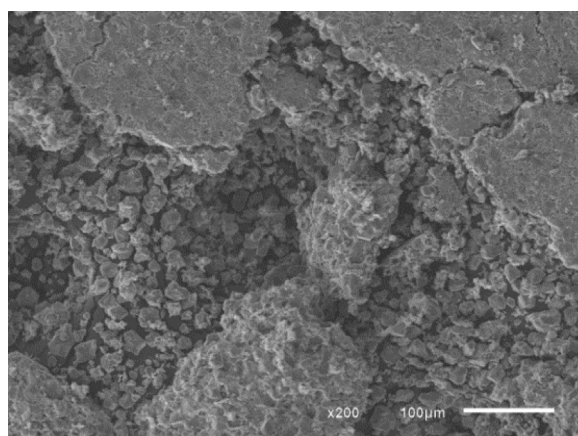
Cubic spinel cobalt oxides are semiconductor materials with good catalytic activity in photocatalysis. UV-light irradiation under semiconductors generates electrons (e[−]) in the conduction bands and holes (h⁺) in the valence band (Eq. (4)). The photogenerated electron-hole pair can oxidize either an organic molecule directly or an H₂O₂ forming hydroxyl radical (•OH) and OH₂•, which can attack adsorbed organic molecules, leading finally to their complete degradation (Eq. (5) and (6)) [27–30]. The total reaction among the Co₃O₄ and LiCoO₂, UV radiation, and H₂O₂ could be written as follows:



(A)



(B)



(C)

Fig. 3. LiCoO_2 cathode material from spent lithium ion batteries: (A) XRD; (B) Raman spectrum; (C) SEM images.

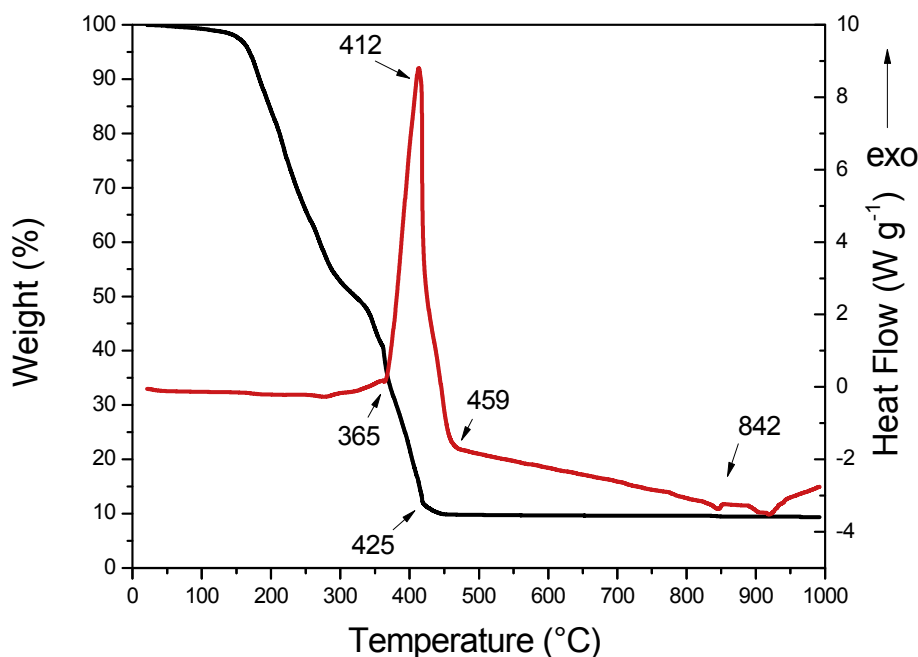


Fig. 4. TG (black plot) and DSC (red plot) analyses of the precursor material. (For interpretation of the references to colour in this figure legend, the reader is referred to the web version of this article.)

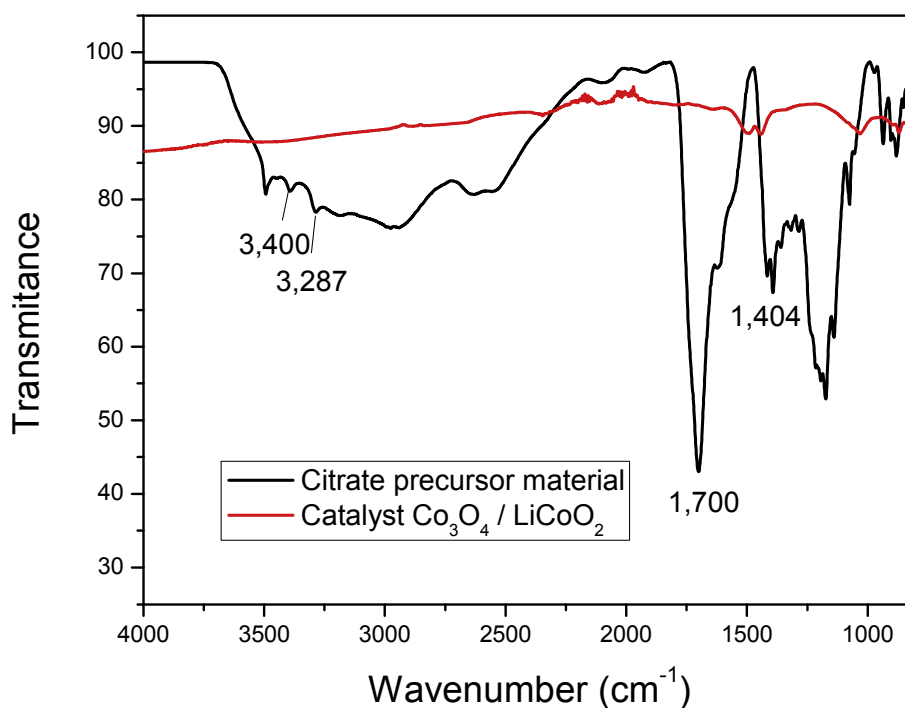
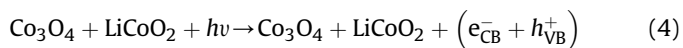
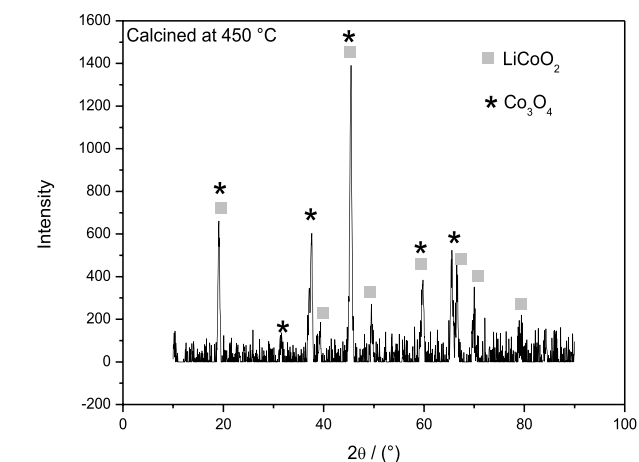


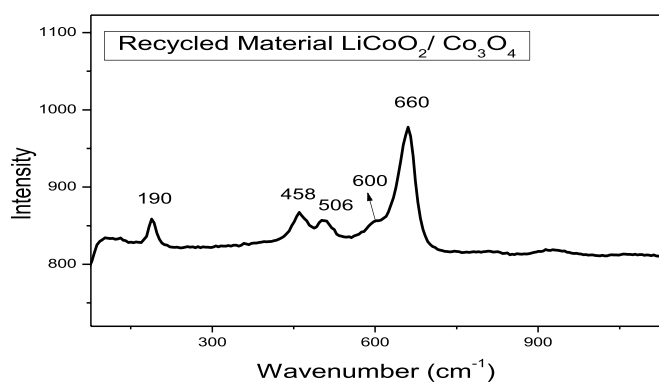
Fig. 5. IR spectra the precursor material and cobalt oxides obtained after precursor material calcination at 450 °C.



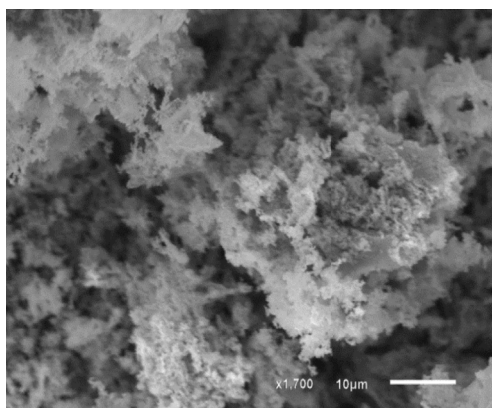
The discoloration of methylene blue dye was monitored by a UV–visible spectrophotometer at wavelengths of 613 nm and 664 nm, as shown in Fig. 7A. The discoloration rate for absorption peaks at 664 nm and 613 nm is shown in Fig. 7B. The absorption peak at 664 nm diminished faster than the peak at 613 nm. This indicates that the demethylation of the dimer occurs faster than the cleavage of aromatic rings [27]. The average discoloration rate ($\mu\text{g/h}$) was calculated as follows:



(A)



(B)

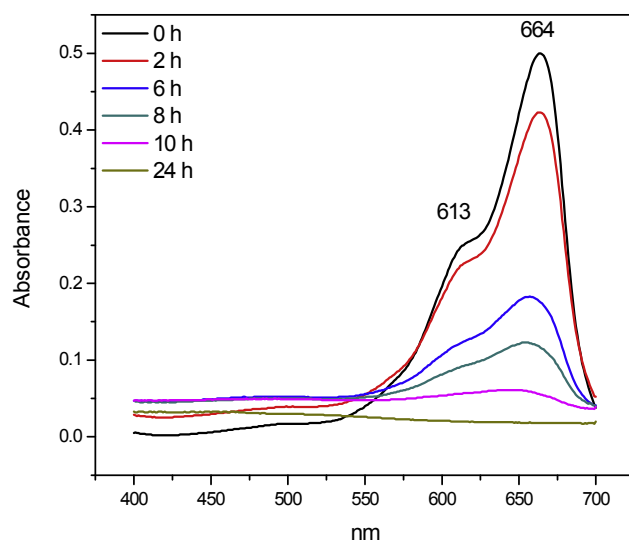


(C)

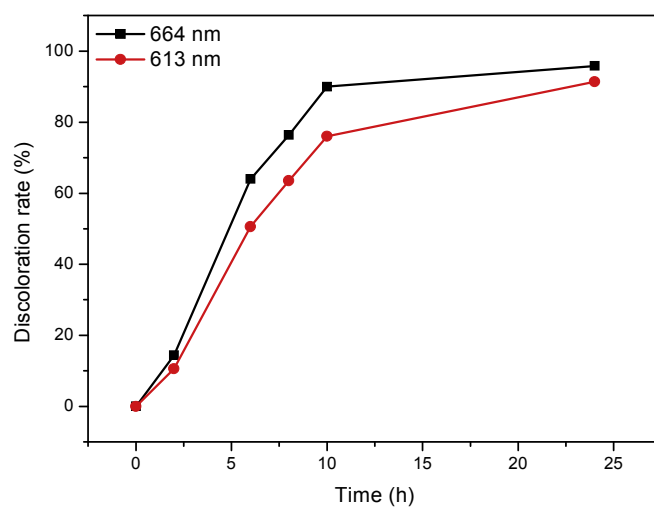
Fig. 6. Recycled material: (A) XRD; (B) Raman spectrum; (C) SEM images.

$$\text{Average discoloration rate} = \frac{C D 1000}{100 \times t} \quad (7)$$

where C is the initial concentration of dye (mgL^{-1}) and D is the dye discoloration (%) after time t (h). In this experiment, the average



(A)



(B)

Fig. 7. A) Dye degradation monitored by UV-spectrophotometry, B) Discoloration rate of methylene blue dye for absorption peak at 664 nm and 613 nm.

discoloration rate after 10 h was $270 \mu\text{gh}^{-1}$.

The catalysis was also subjected to a kinetic analysis of a second-order reaction. Data were analyzed according to the kinetic equation of the second order, given by Eq. (8):

$$\frac{1}{C} = \frac{1}{C_0} - kt \quad (8)$$

where C_0 is the initial concentration of methylene blue, C is the concentration of methylene blue at time t , and k is the rate constant equation.

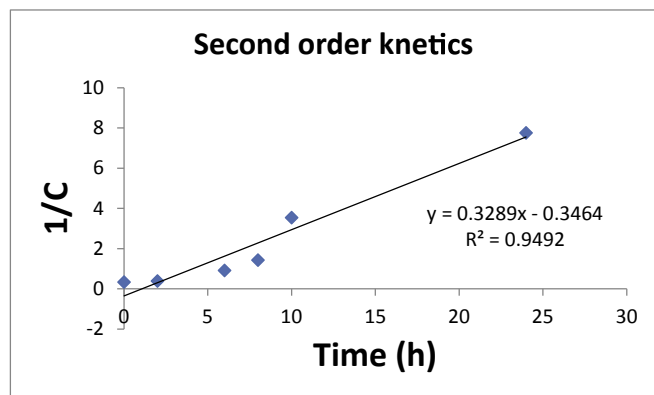


Fig. 8. Kinetics of the methylene blue dye molecule discoloration.

The graph of $1/C$ versus time (t) shown in Fig. 8 has good linearity with $R^2 = 0.9492$, and the rate constant $k = 0.3289 \text{ mol}^{-1}\text{Ls}^{-1}$. The methylene blue dye discoloration is a second-order reaction.

4. Conclusions

In this study, citric acid was used as an organic acid leaching agent in order to develop an eco-friendly recycling route for spent Li-ion batteries. Cobalt and lithium recovered from the leaching solution were used to form a sol-gel material. The precursor material, which was calcined at 450°C , formed a mixture of Co_3O_4 and LiCoO_2 , which was tested as a catalyst of discoloration in methylene blue dye. The total discoloration that occurred indicates that $\text{Co}_3\text{O}_4/\text{LiCoO}_2$ is a promising catalyst. The discoloration of dye molecules in the presence of the catalyst had an efficiency of 90% after 10 h and 100% after 24 h of heterogeneous catalysis. The contribution of this work is that it presents a means to produce valuable materials having catalytic properties from spent Li-ion batteries through an effective recycling process without polluting the environment.

Acknowledgments

The authors acknowledge NCQP, UFES, CAPES, FAPES, Laboratório de Ultraestrutura Celular Carlos Alberto Redins (LUCCAR).

References

- [1] E.M.S. Barbieri, E.P.C. Lima, S.J. Cantarino, M.F.F. Leles, M.B.J.G. Freitas, Recycling of spent ion-lithium batteries as cobalt hydroxide, and cobalt oxide films formed under a conductive glass substrate, and their electrochemical properties, *J. Power Sources* 269 (2014) 158–163, <http://dx.doi.org/10.1016/j.jpowsour.2014.06.162>.
- [2] P.G. Bruce, B. Scrosati, J. Tarascon, Lithium batteries nanomaterials for rechargeable lithium batteries, *Angew. Chem.* 47 (2008) 2930–2946, <http://dx.doi.org/10.1002/anie.200702505>.
- [3] J.W. Fergus, Recent developments in cathode materials for lithium ion batteries, *J. Power Sources* 195 (2010) 939–954, <http://dx.doi.org/10.1016/j.jpowsour.2009.08.089>.
- [4] M.K. Jha, A. Kumari, A.K. Jha, V. Kumar, J. Hait, B.D. Pandey, Recovery of lithium and cobalt from waste lithium ion batteries of mobile phone, *Waste Manag.* 33 (2013) 1890–1897, <http://dx.doi.org/10.1016/j.wasman.2013.05.008>.
- [5] L. Li, J. Ge, R. Chen, F. Wu, S. Chen, X. Zhang, Environmental friendly leaching reagent for cobalt and lithium recovery from spent lithium-ion batteries, *Waste Manag.* 30 (2010) 2615–2621, <http://dx.doi.org/10.1016/j.wasman.2010.08.008>.
- [6] P. Ghosh, S. Mahanty, M.W. Raja, R.N. Basu, H.S. Maiti, Structure and optical absorption of combustion-synthesized nanocrystalline LiCoO_2 , *J. Mater. Res.* 22 (2007) 1162–1167, <http://dx.doi.org/10.1557/jmr.2007.0157>.
- [7] L. Chen, X. Tang, Y. Zhang, L. Li, Z. Zeng, Y. Zhang, Hydrometallurgy process for the recovery of cobalt oxalate from spent lithium-ion batteries, *Hydrometallurgy* 108 (2011) 80–86, <http://dx.doi.org/10.1016/j.hydromet.2011.02.010>.

- [8] G.P. Nayaka, K.V. Pai, J. Manjanna, S.J. Keny, Use of mild organic acid reagents to recover the Co and Li from spent Li-ion batteries, *Waste Manag.* (2015) 8–12, <http://dx.doi.org/10.1016/j.wasman.2015.12.008>.
- [9] L. Li, L. Zhai, X. Zhang, J. Lu, R. Chen, F. Wu, K. Amine, Recovery of valuable metals from spent lithium-ion batteries by ultrasonic-assisted leaching process, *J. Power Sources* 262 (2014) 380–385, <http://dx.doi.org/10.1016/j.jpowsour.2014.04.013>.
- [10] D.C.R. Espinosa, A. Moura, A.J.S. Tenório, An overview on the current processes for the recycling of batteries, *J. Power Sources* 135 (2004) 311–319, <http://dx.doi.org/10.1016/j.jpowsour.2004.03.083>.
- [11] L. Li, J.B. Dunn, X.X. Zhang, L. Gaines, R.J. Chen, F. Wu, K. Amine, Recovery of metals from spent lithium-ion batteries with organic acids as leaching reagents and environmental assessment, *J. Power Sources* 233 (2013) 180–189, <http://dx.doi.org/10.1016/j.jpowsour.2012.12.089>.
- [12] L. Li, J. Ge, F. Wu, R. Chen, S. Chen, B. Wu, Recovery of cobalt and lithium from spent lithium ion batteries using organic citric acid as leachant, *J. Hazard. Mater.* 176 (2010) 288–293, <http://dx.doi.org/10.1016/j.jhazmat.2009.11.026>.
- [13] E.M. Garcia, H.A. Taroco, T. Matencio, R.Z. Domingues, J.A.F. dos Santos, M.B.J.G. de Freitas, Electrochemical recycling of cobalt from spent cathodes of lithium-ion batteries: its application as coating on SOFC interconnects, *J. Appl. Electrochem.* 41 (2012) 1373–1379, <http://dx.doi.org/10.1007/s10800-011-0339-3>.
- [14] E.M.S. Barbieri, E.P.C. Lima, M.F.F. Leles, M.B.J.G. Freitas, Recycling of cobalt from spent Li-ion batteries as $\beta\text{-Co}(\text{OH})_2$ and the application of Co_3O_4 as a pseudocapacitor, *J. Power Sources* 270 (2014) 158–165, <http://dx.doi.org/10.1016/j.jpowsour.2014.07.108>.
- [15] T. Gross, C. Hess, Raman diagnostics of LiCoO_2 electrodes for lithium-ion batteries, *J. Power Sources* 256 (2014) 220–225, <http://dx.doi.org/10.1016/j.jpowsour.2014.01.084>.
- [16] J. Yang, H. Liu, W.N. Martens, R.L. Frost, Synthesis and characterization of Cobalt hydroxide, cobalt oxyhydroxide, and cobalt oxide nanodiscs, *J. Phys. Chem. C* 114 (2010) 111–119, <http://dx.doi.org/10.1021/jp908548f>.
- [17] J.I. Yamaki, Y. Baba, N. Katayama, H. Takatsuki, M. Egashira, S. Okada, Thermal stability of electrolytes with Li_xCoO_2 cathode or lithiated carbon anode, *J. Power Sources* 119–121 (2003) 789–793, [http://dx.doi.org/10.1016/S0378-7753\(03\)00254-4](http://dx.doi.org/10.1016/S0378-7753(03)00254-4).
- [18] E.Z.R. Stoyanova, M. Gorova, Ultrafine layered obtained from citrate precursors, *Ionics (Kiel)* 3 (1997) 1–15.
- [19] E. Zhecheva, R. Stoyanova, M. Gorova, R. Alca, J. Morales, Lithium – cobalt citrate precursors in the preparation of intercalation electrode materials, *Chem. Mater.* 4756 (1996) 1429–1440.
- [20] N. Muchnick, F. Herrera, D. Albuquerque, R. Pastene, J.L. Gautier, Spinel $\text{LiFe}_x\text{Co}_{2-x}\text{O}_4$ ($0.25 \leq x \leq 1$) as cathodes in Lithium batteries. Relationship between ionic distribution and Lithium ion insertion, *J. Chil. Chem. Soc.* 4 (2013) 2005–2010.
- [21] Z. Zhou, Y. Deng, H. Wan, Structural diversities of cobalt (II) coordination 2005, *Cryst. Growth Design* 5 (2005) 1109–1117.
- [22] Y. Gu, D. Chen, X. Jiao, Synthesis and electrochemical properties of nano-structured LiCoO_2 fibers as cathode materials for lithium-ion batteries, *J. Phys. Chem. B* 109 (2005) 17901–17906, <http://dx.doi.org/10.1021/jp0521813>.
- [23] H. Porthault, R. Baddour-Hadjen, F. Le Cras, C. Bourbon, S. Franger, Raman study of the spinel-to-layered phase transformation in sol–gel LiCoO_2 cathode powders as a function of the post-annealing temperature, *Vib. Spectrosc.* 62 (2012) 152–158, <http://dx.doi.org/10.1016/j.vibspec.2012.05.004>.
- [24] C.M. Burba, K.M. Shaju, P.G. Bruce, R. Frech, Infrared and Raman spectroscopy of nanostructured LT- LiCoO_2 cathodes for Li-ion rechargeable batteries, *Vib. Spectrosc.* 51 (2009) 248–250, <http://dx.doi.org/10.1016/j.vibspec.2009.06.002>.
- [25] V.C.B. Pegoretti, P.V.M. Dixini, P.C. Smecellato, S.R. Biaggio, M.B.J.G. Freitas, Thermal synthesis, characterization and electrochemical study of high-temperature (HT) LiCoO_2 obtained from $\text{Co}(\text{OH})_2$ recycled of spent lithium ion batteries, *Mater. Res. Bull.* 86 (2017) 5–9, <http://dx.doi.org/10.1016/j.materresbull.2016.09.032>.
- [26] J. Fu, Y. Bai, C. Liu, H. Yu, Y. Mo, Physical characteristic study of LiCoO_2 prepared by molten salt synthesis method in $550\text{--}800^\circ\text{C}$, *Mater. Chem. Phys.* 115 (2009) 105–109, <http://dx.doi.org/10.1016/j.matchemphys.2008.11.027>.
- [27] T. Warang, N. Patel, R. Fernandes, N. Bazzanella, A. Miotello, Applied Catalysis B: environmental Co_3O_4 nanoparticles assembled coatings synthesized by different techniques for photo-degradation of methylene blue dye, *Appl. Catal. B Environ.* 132–133 (2013) 204–211, <http://dx.doi.org/10.1016/j.apcatb.2012.11.040>.
- [28] I. Poullos, I. Ts, Photodegradation of the textile dye Reactive Black 5 in the presence of semiconducting oxides, *J. Chem. Technol. Biotechnol.* 357 (1999) 349–357.
- [29] Q. Liu, L.C. Wang, M. Chen, Y. Cao, H.Y. He, K.N. Fan, Dry citrate-precursor synthesized nanocrystalline cobalt oxide as highly active catalyst for total oxidation of propane, *J. Catal.* 263 (2009) 104–113, <http://dx.doi.org/10.1016/j.jcat.2009.01.018>.
- [30] Z. Ma, Cobalt oxide catalysts for environmental remediation, *Curr. Catal.* 3 (2014) 15–26.